# PCCP

Accepted Manuscript


This is an *Accepted Manuscript*, which has been through the Royal Society of Chemistry peer review process and has been accepted for publication.

*Accepted Manuscripts* are published online shortly after acceptance, before technical editing, formatting and proof reading. Using this free service, authors can make their results available to the community, in citable form, before we publish the edited article. We will replace this *Accepted Manuscript* with the edited and formatted *Advance Article* as soon as it is available.

You can find more information about *Accepted Manuscripts* in the Information for Authors.

Please note that technical editing may introduce minor changes to the text and/or graphics, which may alter content. The journal's standard Terms & Conditions and the Ethical guidelines still apply. In no event shall the Royal Society of Chemistry be held responsible for any errors or omissions in this *Accepted Manuscript* or any consequences arising from the use of any information it contains.

ROYAL SOCIETY OF CHEMISTRY

www.rsc.org/pccp

# Thermally Activated Long Range Electron Transport in Living Biofilms

Matthew D. Yates[1], Joel P. Golden[1], Jared Roy[2], Sarah M. Strycharz-Glaven[1], Stanislav Tsoi[3], Jeffrey S. Erickson[1], Mohamed Y. El-Naggar[4], Scott Calabrese Barton[5], and Leonard M. Tender[1,*]

[1]Center for Bio/Molecular Science and Engineering, Naval Research Laboratory, Washington, DC, 20375 USA
[2]George Mason University, Fairfax, VA, 22030 USA
[3]Chemistry Division, Naval Research Laboratory, Washington, DC, 20375 USA
[4]Departments of Physics, Biological Sciences, and Chemistry, University of Southern California, Los Angeles, CA, 90089 USA
[5]Department of Chemical Engineering and Materials Science, Michigan State University, East Lansing, MI, 48824 USA

Correspondence and requests for materials should be addressed to L.M.T. (tender@nrl.navy.mil)

M.D.Y.: Postdoctoral fellow, National Research Council, Washington, DC USA 20418

## Abstract

Microbial biofilms grown utilizing electrodes as metabolic electron acceptors or donors are a new class of biomaterials with distinct electronic properties. Here we report that electron transport through living electrode-grown *Geobacter sulfurreducens* biofilms is a thermally activated process with incoherent redox conductivity. The temperature dependency of this process is consistent with electron-transfer reactions involving hemes of *c*-type cytochromes known to play important roles in *G. sulfurreducens* extracellular electron transport. While incoherent redox conductivity is ubiquitous in biological systems at molecular-length scales, it is unprecedented over distances it appears to occur through living *G. sulfurreducens* biofilms, which can exceed 100 microns in thickness.

## Introduction

Extracellular electron transport (EET) is a widespread microbial respiratory strategy that drives global biogeochemical cycles,[1, 2] and is actively investigated for biocatalysis in renewable energy and synthesis technologies.[3] By performing EET, certain microorganisms transport electrons between intracellular metabolic processes and extracellular insoluble electron acceptors or donors ranging from natural minerals to electrodes.[4] For example, the highly studied iron-reducing bacterium *G. sulfurreducens* can utilize insoluble iron (oxy)hydroxides as electron acceptors, providing it a distinct metabolic niche in otherwise oxidant-scarce environments. When grown using acetate as a metabolic electron donor and an electrode poised at a sufficiently positive potential to act as an inexhaustible metabolic electron acceptor, *G. sulfurreducens* forms a multi-cell thick biofilm on the electrode surface comprised of cells and secreted extracellular substances that include biopolymers, protein filaments, and redox proteins.[5] Electrons resulting from intracellular oxidation of acetate are transported to outer surfaces of cells and through the biofilm to the electrode surface over distances that can exceed 100 microns.[6] In this living system the *G. sulfurreducens* cells catalyze electrode oxidation of acetate, conserving a portion of the liberated energy to satisfy their energy needs; the extracellular substances act as a conducting matrix electrically connecting cells to the electrode surface;[7] and catalytic current collected by the electrode is proportional to the net rate of acetate turnover by the cells. While electrode-grown *G. sulfurreducens* biofilms have received considerable attention,[8-13] the mechanisms underlying the nature of their conductivity remain debated.[14, 15] A mechanistic understanding is further motivated by the recent demonstration of microbial bioelectrodes, such as those that catalyze electrode reduction of nitrate[16] and carbon dioxide,[17, 18] and recent observations

indicating possible centimeter length-scale electron transport through multi-cellular microbial cable assemblies.[19]

Two incongruent mechanisms have been proposed to describe EET occurring through electrode-grown *G. sulfurreducens* biofilms. One mechanism, thought to be specific to *G. sulfurreducens*, invokes coherent metallic-like conductivity similar to that of organic semiconductors attributed to π-stacking of aromatic residues of PilA subunits of type IV pili (a type of protein filament).[20, 21] The other mechanism invokes incoherent redox conductivity[22, 23] similar to that of redox polymers[24] stemming from sequential, thermally activated electron transfer reactions among immobilized redox cofactors, which are thought to be hemes of outer membrane or extracellular *c*-type cytochromes known to play central roles in extracellular electron transfer by *G. sulfurreducens* and other organisms.[25-28] Resolving the specific contributions of *c*-type cytochromes and type IV pili to EET of electrode-grown *G. sulfurreducens* biofilms has been confounded by the role type IV pili play in surface attachment, secretion, and extracellular localization of *c*-type cytochromes; [29, 30] the lack of analytical techniques with sufficient resolution to provide definitive information regarding spatial organization of *c*-type cytochromes within *G. sulfurreducens* biofilms; and results in which deletion of *pilA* or certain types of *c*-type cytochromes only partially inhibits EET by *G. sulfurreducens* to iron (oxy)hydroxides and electrodes.[31]

Temperature is an experimentally tractable parameter for which the two proposed mechanisms predict very different dependencies: coherent metallic-like conductivity increases with decreasing temperature, whereas incoherent redox conductivity decreases with decreasing temperature.[20] Thus far, the only reported temperature dependency

measurements of electrical conductivity of electrode-grown *G. sulfurreducens* biofilms have been of the mutant strain CL-1,[20] in which a gene containing a putative PilZ domain (involved in type IV pili biogenesis) was deleted, significantly altering the extracellular matrix, abundance of PilA protein, abundance of at least two types of extracellular *c*-type cytochromes, and turnover current compared to the wild type strain.[32] Moreover, these measurements were not performed on living biofilms, but rather performed *ex situ* under vacuum on non-living biofilms peeled off of the electrodes on which they were grown.

Here we report results of *in situ* electrical conductivity measurements performed at different temperatures on living electrode-grown wild-type *G. sulfurreducens* biofilms. The conductivity of the biofilms decreases with decreasing temperature and exhibits an Arrhenius behavior, which supports a redox gradient driven mechanism of EET. Fitting the data to the Arrhenius equation yielded activation and reorganizational energies consistent with electron self-exchange among *c*-type cytochromes acting as the charge carriers.

## Results and Discussion

The electrical conductivity of living electrode-grown wild type *G. sulfurreducens* biofilms decreases with decreasing temperature (Fig. 1A). Fitting the temperature dependency of conductivity to the Arrhenius rate expression (Fig. 1B) yields an activation energy ($E_a$) of 0.13 ± 0.02 eV and a reorganizational energy ($\lambda = 4E_a$)[33] of 0.52 ± 0.08 eV, consistent with electron transfer reactions involving hemes of *c*-type cytochromes.[34-37] These measurements were performed at different temperatures in the same aqueous medium and under conditions at which *G. sulfurreducens* biofilms are

typically grown and studied. Measurements were performed using interdigitated microelectrode arrays (IDA) – a 2-electrode configuration comprised of 2 interdigitated electrodes (source and drain) used extensively to characterize conductivity of polymer films[38, 39] – on which stationary phase *G. sulfurreducens* biofilms were grown (Fig. 2; Experimental replicates depicted in Supplementary Fig. S3-5).[22, 23] Conductivity at 30°C, the temperature at which *G. sulfurreducens* biofilms are typically grown and studied, was unaffected by changing the temperature to 10°C and then back to 30°C (Fig. 1A and 1B), indicating that the effect was reversible over this temperature range. Source-drain currents measured upon cooling and heating are both plotted in Fig. 1A and 1B and are statistically indistinguishable from one another. These measurements were performed at a fixed gate potential to eliminate background current due to biofilm Faradic charging (discussed below) and in the absence of acetate (non-turnover condition) to eliminate background current due to acetate oxidation by cells in the biofilm (i.e., turnover current). When placed back under turnover condition at 30°C the biofilm resumed generating catalytic current at the same level as before these measurements were made, indicating that the biofilm was not adversely affected by the temporary change in temperature or by the temporary removal of acetate. (Supplementary Fig. S6).

In the case of an ideal redox conductor:[22, 24]

Eqn. 1 $$I_{SD} = nFDSC[P_S - P_D]$$

Eqn 2. $$P_S = \frac{1}{1+e^{\left[\frac{nF}{RT}\left(E_G - \frac{V_{SD}}{2} - E^{o'}\right)\right]}}$$

Eqn 3. $$P_D = \frac{1}{1+e^{\left[\frac{nF}{RT}\left(E_G + \frac{V_{SD}}{2} - E^{o'}\right)\right]}}$$

Eqn. 4 $$E_G = \frac{(E_D + E_S)}{2}$$

Eqn. 5 $$V_{SD} = E_D - E_S$$

Eqn. 6 $$D = \frac{k_{ex} C \delta^2}{6}$$

Eqn. 7 $$k_{ex} = Ae^{-E_a/kT}$$

where $E_S$ and $E_D$ are potentials applied to the source and drain; $I_{SD}$ is the resulting source-drain current (proportional to the rate of electron transport (ET) through the material from the source to the drain); $E_G$ is gate potential (average of source and drain potentials); $V_{SD}$ is source-drain voltage (difference between drain and source potentials); $P_S$ and $P_D$ are probabilities that cofactors involved in the heterogeneous electron transfer reactions (across the 2 biofilm/electrode interfaces) are reduced (can donate an electron) vs. oxidized (can accept an electron), which range from 0 (all are oxidized) to 1 (all are reduced); $T$ is temperature; $n$ is the number of electrons transferred per electron transfer reaction (n = 1)[40]; $F$, $R$, *and* $k$ are the Faraday, gas, and Boltzmann constants; $S$ is a geometric factor dependent on the electrode configuration and material thickness numerically determined to be 14.5 cm for the specific IDAs and biofilms examined here (Supplementary Information); $D$ is the effective diffusion coefficient for electrons in the material[24, 41]; $C$, $\delta$, and $E^{o'}$ are the redox cofactor concentration, spacing, and formal potential; and $k_{ex}$, $A$, and $E_a$ are the rate constant, frequency factor, and activation energy for electron transfer reactions between cofactors. Eqn. 1 is analogous to Fick's 1st law of diffusion. In the case of a redox conductor, application of source and drain potentials induces a redox gradient – a gradient of reduced (or oxidized) cofactors on which electrons (or holes) momentarily reside during ET – across the material between the

electrodes. The magnitude of the resulting source-drain current is proportional to the magnitude of this redox gradient, which is proportional to $SC[P_S - P_D]$.[24] (See Supplementary Information for a description of Eqn. 1-7).

Eqn. 1 predicts that redox conductors should exhibit a peak-shaped dependency of source-drain current on gate potential centered at $E_G = E^{o'}$ when a constant source-drain voltage is maintained across the electrodes (electrochemical gating measurements, (Supplementary Fig. S7). The peak-shaped dependency of source-drain current on gate potential observed here (Fig. 3A) sharply contrasts the sigmoid-shaped dependency exhibited by organic semiconductors such as poly(3-methyl thiophene)[38] and is strong evidence that redox conductivity occurs in living, electrode-grown *G. sulfurreducens* biofilms.[42] It also sharply contrasts with a previous electrochemical gating study, which is based on results acquired with methods that have been called into question,[43] that finds living, electrode-grown *Geobacter sulfurreducens* biofilms to be metallic-like conductors.[20]

The redox cofactor formal potential indicated by Fig. 3A (-0.390 V vs. Ag/AgCl) is consistent with formal potentials of redox cofactors in living, electrode-grown *G. sulfurreducens* biofilms determined by spectroelectrochemical methods to be *c*-type cytochromes.[12, 44, 45] Visualization using immuno-gold labeling of three different *c*-type cytochromes proposed to be involved in EET of electrode-grown *G. sulfurreducens* biofilms indicates that these proteins were distributed throughout the biofilms, associated with cell membranes and the extracellular polysaccharide matrix.[32, 50, 51] Antibody size and label efficiency, however, precludes immuno-gold labeling from determining whether these *c*-type cytochromes are spaced close enough (< 2 nm) for redox

conductivity to occur.[52] The genome of *G. sulfurreducens* potentially encodes over 100 different *c*-type cytochromes many of which have yet to be identified and experimentally evaluated for involvement in EET. The apparent redox cofactor formal potential nearly coincides with the catalytic midpoint potential ($E_M$) indicated by turnover voltammetry performed on the same biofilm (Fig. 3C).[46] This suggests that the same cofactors are involved in EET for source-drain current, when an electrode is the source of electrons, as for turnover current, when acetate turnover by cells is the source of electrons.[46] Current peaks wider than predicted by Eqn. 1 are consistent with a distribution in formal potentials of redox cofactors involved in EET (Supplementary Fig. S7).[23]

For the electrochemical gating measurements performed here, the source-drain voltage is sufficiently small ($V_{SD} \leq 0.05$ V (Supplementary Fig. S8) that Eqn. 1 can be linearly approximated by Ohm's Law:

Eqn. 8 $$I_{SD} = GV_{SD}$$

Eqn. 9 $$G = \sigma S$$

where $G$ is conductance and $\sigma$ is conductivity, such that conductivity scales linearly with experimentally measured source-drain current (scaling factor = $1/V_{SD}S = 6.90$ cm$^{-1}$ V$^{-1}$ for $S = 14.50$ cm and $V_{SD} = 0.01$ V, used to scale right-hand vertical axes of Fig. 1 and 3). For an ideal redox conductor:

Eqn. 10 $$\sigma = \frac{n^2F^2DC}{RT}\left(\frac{e^{\left[\frac{nF}{RT}(E_G-E^{o'})\right]}}{1+2e^{\left[\frac{nF}{RT}(E_G-E^{o'})\right]}+e^{\left[\frac{2nF}{RT}(E_G-E^{o'})\right]}}\right)$$

obtained by linearly approximating Eqn. 1 for the case of a sufficiently small source-drain voltage for which Eqn.8 applies (Supplementary Information). When the gate potential is equal to the formal potential ($E_G = E^o$'), Eqn. 10 can be expressed as:

Eqn. 11 $$\sigma = \frac{X}{T} e^{-E_a/kT}$$

Eqn. 12 $$X = \frac{n^2 F^2 C^2 \delta^2 A}{24R}$$

where $X$ is a temperature independent constant. Fitting temperature dependency of $\sigma$ when $E_G = E^o$' based on Eqn. 11 is expected to yield the activation energy for the redox cofactor electron self-exchange reaction (Fig. 1B). The maximum conductivity at 30$^o$C is on the order of $10^{-6}$ S cm$^{-1}$ (Fig. 3A). This conductivity corresponds to electron mobilities orders of magnitude below the lower limit of coherent band transport, further ruling out that the mechanism of biofilm transport is similar to π-stacked materials and organic semiconductors.[47, 48]

Regardless of the assumed mechanism of EET, *G. sulfurreducens* biofilms possess intrinsic redox activity in which a change in gate potential induces a net change in oxidation state of electrode-accessible redox cofactors throughout the biofilm (i.e., Faradaic charging),[5] which occurs through a combination of heterogeneous EET (across the biofilm/electrode interfaces) and homogenous EET (within the biofilm). This process results in voltammetric current peaks observed under non-turnover condition (when not obscured by acetate turnover current) that scale linearly with the square root of scan rate and that exhibit negligible splitting with increasing scan rate (Fig. 4A). A net change in oxidation state of biofilm redox cofactors also results in current transients that decay with

the square root of time when the gate potential is abruptly changed under non-turnover condition (Fig. 4B) across the cofactor formal potential. Both results are observed for redox conductors[41, 49] and are consistent with non-limiting heterogeneous electron transfer and with diffusive homogeneous electron transport occurring in *G. sulfurreducens* biofilms described by Eqn. 1.[41]

## Conclusions

The results described here provide strong evidence that living electrode-grown *G. sulfurreducens* biofilms act as redox conductors in which hemes of *c*-type cytochromes are the apparent redox cofactors involved in EET. Redox conduction over distances only recently determined to occur in electrode-grown in *G. sulfurreducens* biofilms is unprecedented in biological systems based on classical molecular-scale redox reactions. However, long-range redox conduction may be prevalent in biological systems,[19, 53] and understanding this process provides a framework for increased understanding of environmental nutrient cycling and potential for biotechnology applications.

## Materials and Methods

Unless otherwise noted methods and materials used here were the same as previously reported.[7, 23]

**Interdigitated microelectrode arrays**.

IDAs (interdigitated microelectrode arrays), used extensively to perform conductivity measurements on electrochemically grown polymers,[38, 39, 54] are a variation of the double-band electrode configuration (see Fig. 1a, Kankare and Kupila (1992)[55] and

Fig. 2b of Snider et al. (2012)[23]). The IDAs used to obtain data depicted in Figs. 1-4 were obtained commercially (CH Instruments, model 012125) and consist of 130 parallel gold rectangular bands, each 2 mm long x 10 µm wide x 90 nm thick, patterned onto a flat glass substrate separated by 5 µm wide gaps (total electrode area (source + drain): 0.026 $cm^2$, total biofilm coated array area (electrodes and gap): 0.039 $cm^2$). Every other band is electrically connected at opposite ends of the array forming two separately addressable interdigitated electrodes, each comprised of 65 bands, separated by a single 25.8 cm long (129 x 2mm) x 5 µm wide gap that weaves back and forth across the array. IDAs were used as received. Teflon insulated wires were affixed to the terminal contact pads of the IDA working electrodes using conductive silver epoxy (Electron Microscopy Sciences, Hatfield, PA). These connections were then sealed in Scotchcast resin (3M, Austin, TX) using the tip of a 15-ml conical centrifuge tube as a mold. IDAs used to obtain replicate data depicted in supplementary Figs. S3-5 were identical to those described above, or fabricated in house following previous methods.[7, 23]

**Electrochemical Instrumentation.**

WaveDriver bipotentiostats Model WD20 (Pine Instruments, Durham, NC) were used to perform all experiments presented in Fig 1-4 except for the potential step experiments (Fig. 4B), which were performed using a Biologic VMP3 8-channel potentiostat (Biologic Inc., Knoxville, TN).

**Electrochemical reactors.**

All biofilm electrochemical experiments were performed in 250-ml water jacketed electrochemical reactors (Pine Instruments, Durham, NC) maintained under anaerobic conditions by constant sparging with an 80% $N_2$/ 20% $CO_2$ gas mix. Reactors

contained a Ag/AgCl reference electrode (3M NaCl, Bioanalytical Systems, Inc.) and a non-limiting graphite rod counter electrode (0.6 mm dia, 10 mm length, Electron Microscopy Sciences) as previously described.[22, 23] All potentials reported here are vs. Ag/AgCl (3M NaCl) and can be approximated as vs. SHE by addition of 0.195 V. Temperature was controlled using a Haake AC200 temperature controller (Thermo Scientific) to circulate temperature regulated water through the jackets of the electrochemical reactors. Temperature regulation of the experimental reactors was verified using a glass thermometer upstream in the circulator and a glass thermometer downstream in a second reactor.

**Biofilm growth.**

Biofilms were grown at 30°C on IDAs covering the electrode bands and gaps by poising both electrodes at 0.300 V in fresh water media (ATCC 2260, excluding Wolfe's vitamins) containing acetate (10 mM) as the electron donor and carbon source using previously described methods.[22, 23] This resulted in an increase in acetate turnover (catalytic) current over time at both electrodes due to proliferation of cells coupling oxidation of acetate (respiration) with EET to the electrode surfaces.[7, 22, 23, 46] Biofilms were allowed to grow until turnover current plateaued (biofilm stationary phase; approximately10 days after inoculation). Biofilm thickness (80 ± 9 μm) was determined *ex situ* by confocal microscopy as previously described (Supplementary Fig. S9).[23] Electrochemical gating measurements were performed on 3 biological replicates and the results depicted in Fig. 1 and 3 are considered typical.

**Electrochemical gating measurements:**

Electrochemical gating measurements (Fig. 3) were performed at 30°C in the same electrochemical reactors in the same medium used for biofilm growth to ensure biofilm viability. Measurements were performed using the bipotentiostat to simultaneously scan potentials of the source and drain electrodes, and thus gate potential ($E_G$, Eq. 4), at the same scan rate ($v$) while maintaining a constant potential offset between the electrodes (source-drain voltage, $V_{SD}$, Eq. 5) and to measure the source-drain current ($I_{SD}$) separately at each electrode. It was determined that for $v < 2$ mV/s, source-drain current is nearly independent of $v$, for which source-drain current at each gate potential can be considered to be nearly steady state (Supplementary Fig. S5). For all electrochemical gating measurements depicted here $v = 1$ mV/s. It was also determined that for $V_{SD} < 0.2$ V, source-drain current scales linearly with $V_{SD}$ per Eqn. 8 (Supplementary Fig. S8). For all electrochemical gating measurements depicted here $V_{SD} = 0.01$ V. Electrochemical gating measurements were performed with acetate present as during biofilm growth (turnover condition), and after media containing acetate in the electrochemical reactor was replaced with media lacking acetate (non-turnover condition).

When performing electrochemical gating measurements (Fig. 3, Fig. S1), at least two types of background current need to be subtracted from current measured at the source and drain electrodes to yield the source-drain current at each gate potential (Supplementary Fig. S1). The first is current due to intrinsic redox activity of the biofilm in which the oxidation state of redox cofactors changes as gate potential changes (i.e., Faradaic charging current). The second is turnover current due to acetate oxidation, which is expected to occur only under turnover condition. The total background current under both conditions was approximated by sweeping the gate potential at 1 mV/s as

above, but with $V_{SD}$ = 0 V such that $I_{SD}$ = 0 (equivalent to simultaneously performing turnover voltammetry when acetate is present and non-turnover voltammetry when acetate is removed at each electrode). The resulting current at each electrode at each gate potential, which constitutes total background current under each condition, was subtracted from current measured at each electrode for $V_{SD}$ = 0.01V at each gate potential, yielding source-drain current at each electrode for each gate potential (Fig. 3 and Supplementary Fig. S1). Alternatively, subtracting the raw source current directly from the raw drain current yields twice the background subtracted source-drain current, since background currents are expected to be equal at both electrodes and source-drain currents are expected to be equal in magnitude at both electrodes, but opposite in sign (Fig. S2). Both methods of background subtraction were used here. Following all non-turnover measurements, turnover current resumed at previous levels after replacement of media lacking acetate with media containing acetate, indicating biofilm viability throughout the measurements (Supplementary Fig. S6).

The methods used here of slowly sweeping the gate potential with $V_{SD}$ = 0.01 and either subtracting background current obtained at $V_{SD}$ = 0, or subtracting the source from drain current, have been compared to a method in which the gate potential was stepped in 0.05 V increments across the same potential range under non-turnover condition while maintaining $V_{SD}$ = 0.01 V, and recording the source and drain current after sufficient time had elapsed after each step (~2.5 minutes), so that the current achieved a near steady state value.[43] Ideally, current due to Faradaic charging is expected to decay over time following each step as the net oxidation state of cofactors in the biofilm are expected to converge to the gate potential-dependent value. Under non-turnover condition, this

method is expected to directly yield the source-drain current at each electrode. The peak shaped conductivity vs. gate potential dependency obtained by incrementally stepping the gate potential correlated with that obtained by sweeping the gate potential.[43] The peak magnitude however was approximately 2-fold greater for stepping the gate potential than for sweeping the gate potential, which we attribute to persistent Faradaic charging current. We chose to use the sweeping method because it is less tedious, less prone to human error since data collection can be fully automated, and because it provides greater resolution with respect to gate potential. Moreover, when we performed electrochemical gating measurements of a known redox conducting polymer and known semiconducting polymer by slowly sweeping the gate potential and either subtracting current obtained at $V_{SD} = 0$, or subtracting the source from drain current, we obtained the expected results based on prior literature results validating our experimental methods.[43]

**Temperature-dependent conductivity measurements:**

Measurement of the temperature dependency of conductivity (Fig. 1A) of living electrode-grown *G. sulfurreducens* biofilms was performed by stepping the temperature from 30°C to 10°C in 2°C increments under non-turnover condition. The electrodes used in these measurements (IDA source and drain) were the same ones used to grow the biofilms. The gate potential was fixed at -0.390 V vs. Ag/AgCl, the gate potential for which conductivity was determined to be greatest (Fig. 3). Since the gate potential was fixed, there was no background current due to Faradaic charging to contend with. Current was allowed to stabilize at each temperature after the downstream thermometer indicated the desired temperature (>20 minutes). The temperature was then stepped in 10°C increments back to 30°C and conductivity measured again at 20°C and 30°C to confirm

that the effect of temperature on conductivity was reversible. Source-drain currents measured upon cooling and heating are both plotted in Fig. 1A and 1B and are statistically indistinguishable from one another. Electrochemical reactors were not stirred during these measurements to minimize electrical noise. Following these measurements, the biofilms were placed back under turnover condition and turnover current resumed at prior levels confirming that the biofilms were not adversely affected (Supplementary Fig. S6).

Activation energy ($E_a$) was determined by fitting the experimental data to Eqn. 11 to $ln(\sigma T_i)$ *vs.* $1/T_i$, where $i$ is the index for the discrete experimental points. Fitting the experimental data to a straight line using the least squares method with weighted errors given by $1/\sigma_i$ yielded parameters $ln(A)$ and $E_a$. Separate fits were applied to the source and drain data. The corresponding reorganizational energy ($\lambda$) was determined by $\lambda = 4E_a$ following Marcus[33]. Temperature dependency of conductivity measurements were performed on 3 biological replicates and the results depicted in Fig. 1 are considered typical (Supplementary Fig. S4-5).

## References


.1. K. H. Nealson, A. Belz and B. McKee, *Antonie Van Leeuwenhoek International Journal of General and Molecular Microbiology*, 2002, **81**, 215-222.

2. D. R. Lovley, *Annual Reviews of Microbiology*, 1993, **47**, 263-290.

3. B. E. Logan, *Nat. Rev. Microbiol.*, 2009, **7**, 375-381.

4. J. A. Gralnick and D. K. Newman, *Mol. Microbiol.*, 2007, **65**, 1-11.

5. S. M. Strycharz-Glaven and L. M. Tender, *ChemSusChem*, 2012, **5**, 1106-1118.

6. D. R. Bond, S. M. Strycharz-Glaven, L. M. Tender and C. I. Torres, *ChemSusChem*, 2012, **5**, 1099-1105.

7. S. M. Strycharz-Glaven, J. Roy, D. Boyd, R. Snider, J. S. Erickson and L. M. Tender, *ChemElectroChem*, 2014, **1**, 1957-1965.

8. X. Zhu, M. D. Yates and B. E. Logan, *Electrochemistry Communications*, 2012, **22**, 116-119.

9. P. S. Jana, K. Katuri, P. Kavanagh, A. Kumar and D. Leech, *Physical Chemistry Chemical Physics*, 2014, **16**, 9039-9046.

10. Y. Liu and D. R. Bond, *ChemSusChem*, 2012, **5**, 1047-1053.

11. C. E. Levar, C. H. Chan, M. G. Mehta-Kolte and D. R. Bond, *mBio*, 2014, **5**.
12. L. Robuschi, J. Pablo Tomba, G. D. Schrott, P. Sebastian Bonanni, P. Mariela Desimone and J. Pablo Busalmen, *Angewandte Chemie-International Edition*, 2013, **52**, 925-928.
13. P. S. Bonanni, D. F. Bradley, G. D. Schrott and J. P. Busalmen, *ChemSusChem*, 2013, **6**, 711-720.
14. N. S. Malvankar, M. T. Tuominen and D. R. Lovley, *Energy & Environmental Science*, 2012.
15. S. M. Strycharz-Glaven and L. M. Tender, *Energy & Environmental Science*, 2012, **5**, 6250-6255.
16. R. M. S. Kyla P. Gregoire, Leonard M. Tender *Manuscript in preperation*.
17. Z. Wang, D. H. Leary, A. P. Malanoski, R. W. Li, W. J. Hervey, B. J. Eddie, G. S. Tender, S. G. Yanosky, G. J. Vora, L. M. Tender, B. Lin and S. M. Strycharz-Glaven, *Applied and Environmental Microbiology*, 2015, **81**, 699-712.
18. C. W. Marshall, D. E. Ross, E. B. Fichot, R. S. Norman and H. D. May, *Applied and Environmental Microbiology*, 2012, **78**, 8412-8420.
19. C. Pfeffer, S. Larsen, J. Song, M. Dong, F. Besenbacher, R. L. Meyer, K. U. Kjeldsen, L. Schreiber, Y. A. Gorby, M. Y. El-Naggar, K. M. Leung, A. Schramm, N. Risgaard-Petersen and L. P. Nielsen, *Nature*, 2012, **491**, 218-221.
20. N. S. Malvankar, M. Vargas, K. P. Nevin, A. E. Franks, C. Leang, B. C. Kim, K. Inoue, T. Mester, S. F. Covalla, J. P. Johnson, V. M. Rotello, M. T. Tuominen and D. R. Lovley, *Nat. Nanotechnol.*, 2011, **6**, 573-579.
21. M. Vargas, N. S. Malvankar, P. L. Tremblay, C. Leang, J. A. Smith, P. Patel, O. Synoeyenbos-West, K. P. Nevin and D. R. Lovley, *mBio*, 2013, **4**.
22. S. M. Strycharz-Glaven, R. M. Snider, A. Guiseppi-Elie and L. M. Tender, *Energy & Environmental Science*, 2011, **4**, 4366-4379.
23. R. M. Snider, S. M. Strycharz-Glaven, S. D. Tsoi, J. S. Erickson and L. M. Tender, *Proceedings of the National Academy of Sciences of the United States of America*, 2012, **109**, 15467-15472.
24. E. F. Dalton, N. A. Surridge, J. C. Jernigan, K. O. Wilbourn, J. S. Facci and R. W. Murray, *Chem. Phys.*, 1990, **141**, 143-157.
25. C. Leang, M. Coppi and D. Lovley, *J. Bacteriol.*, 2003, **185**, 2096-2103.
26. T. Mehta, M. Coppi, S. E. Childers and D. Lovley, *Appl. Environ. Microb.*, 2005, **71**, 8634-8641.
27. K. P. Nevin, B. C. Kim, R. H. Glaven and J. P. Johnson, *PLoS ONE*, 2009, **4**, e5628.
28. T. C. Santos, M. A. Silva, L. Morgado, J. M. Dantas and C. Salgueiro, *Dalton Transactions*, 2015.
29. C. Leang, X. Qian, T. Mester and D. R. Lovley, *Applied and Environmental Microbiology*, 2010, **76**, 4080-4084.
30. L. V. Richter, S. J. Sandler and R. M. Weis, *Journal of bacteriology*, 2012, **194**, 2551-2563.
31. J. A. Smith, P. L. Tremblay, P. M. Shrestha, O. L. Snoeyenbos-West, A. E. Franks, K. P. Nevin and D. R. Lovley, *Applied and Environmental Microbiology*, 2014, **80**, 4331-4340.
32. C. Leang, N. S. Malvankar, A. E. Franks, K. P. Nevin and D. R. Lovley, *Energy & Environmental Science*, 2013, **6**, 1901-1908.
33. R. A. Marcus, *Journal of Chemical Physics*, 1965, **43**, 679-&.
34. H. S. Byun, S. Pirbadian, A. Nakano, L. Shi and M. Y. El-Naggar, *ChemElectroChem*, 2014, **1**, 1932-1939.
35. A. El Kasmi, J. M. Wallace, E. F. Bowden, S. M. Binet and R. J. Linderman, *J. Am. Chem. Soc.*, 1998, **120**, 225-226.
36. M. Breuer, K. M. Rosso and J. Blumberger, *Proceedings of the National Academy of Sciences*, 2014, **111**, 611-616.
37. C. A. Bortolotti, M. E. Siwko, E. Castellini, A. Ranieri, M. Sola and S. Corni, *J. Phys. Chem. Lett.*, 2011, **2**, 1761-1765.
38. M. J. Natan and M. S. Wrighton, *Progress in Inorganic Chemistry*, 1990, 391-494.
39. C. E. Chidsey, B. J. Feldman, C. Lundgren and R. W. Murray, *Anal. Chem.*, 1986, **58**, 601-607.
40. R. A. Yoho, S. C. Popat and C. I. Torres, *ChemSusChem*, 2014, **7**, 3413-3419.
41. J. W. Gallaway and S. A. Calabrese Barton, *J. Am. Chem. Soc.*, 2008, **130**, 8527-8536.
42. N. S. Malvankar, M. T. Tuominen and D. R. Lovley, *Energy & Environmental Science*, 2012, **5**, 8651-8659.
43. M. D. Yates, S. M. Strycharz-Glaven, J. P. Golden, J. Roy, S. Tsoi, J. S. Erickson, M. Y. El-Naggar, S. C. Barton and L. M. Tender, *Nat. Nanotechnol.*, in review.
44. Y. Liu, H. Kim, R. R. Franklin and D. R. Bond, *ChemPhysChem*, 2011, **12**, 2235-2241.

45. N. Lebedev, S. M. Strycharz-Glaven and L. M. Tender, *ChemPhysChem*, 2014, **15**, 320-327.
46. S. M. Strycharz, A. P. Malanoski, R. M. Snider, H. Yi, D. R. Lovley and L. M. Tender, *Energy Environ. Sci.*, 2011, **4**, 896-913.
47. S. Pirbadian and M. Y. El-Naggar, *Physical chemistry chemical physics : PCCP*, 2012, **14**, 13802-13808.
48. N. F. Polizzi, S. S. Skourtis and D. N. Beratan, *Faraday Discussions*, 2012, **155**, 43-61.
49. R. J. Forster, D. A. Walsh, N. Mano, F. Mao and A. Heller, *Langmuir*, 2004, **20**, 862-868.
50. K. Inoue, C. Leang, A. E. Franks, T. L. Woodard, K. P. Nevin and D. R. Lovley, *Environmental Microbiology Reports*, 2011, **3**, 211-217.
51. C. S. Stephen, E. V. LaBelle, S. L. Brantley and D. R. Bond, *Plos One*, 2014, **9**, e104336-e104336.
52. J. R. Winkler and H. B. Gray, *J. Am. Chem. Soc.*, 2014, **136**, 2930-2939.
53. S. Pirbadian, S. E. Barchinger, K. M. Leung, H. S. Byun, Y. Jangir, R. A. Bouhenni, S. B. Reed, M. F. Romine, D. A. Saffarini, L. Shi, Y. A. Gorby, J. H. Golbeck and M. Y. El-Naggar, *Proceedings of the National Academy of Sciences*, 2014, **111**, 12883-12888.
54. A. Aoki and A. Heller, *Journal of Physical Chemistry*, 1993, **97**, 11014-11019.
55. J. Kankare and E. L. Kupila, *J. Electroanal. Chem.*, 1992, **322**, 167-181.

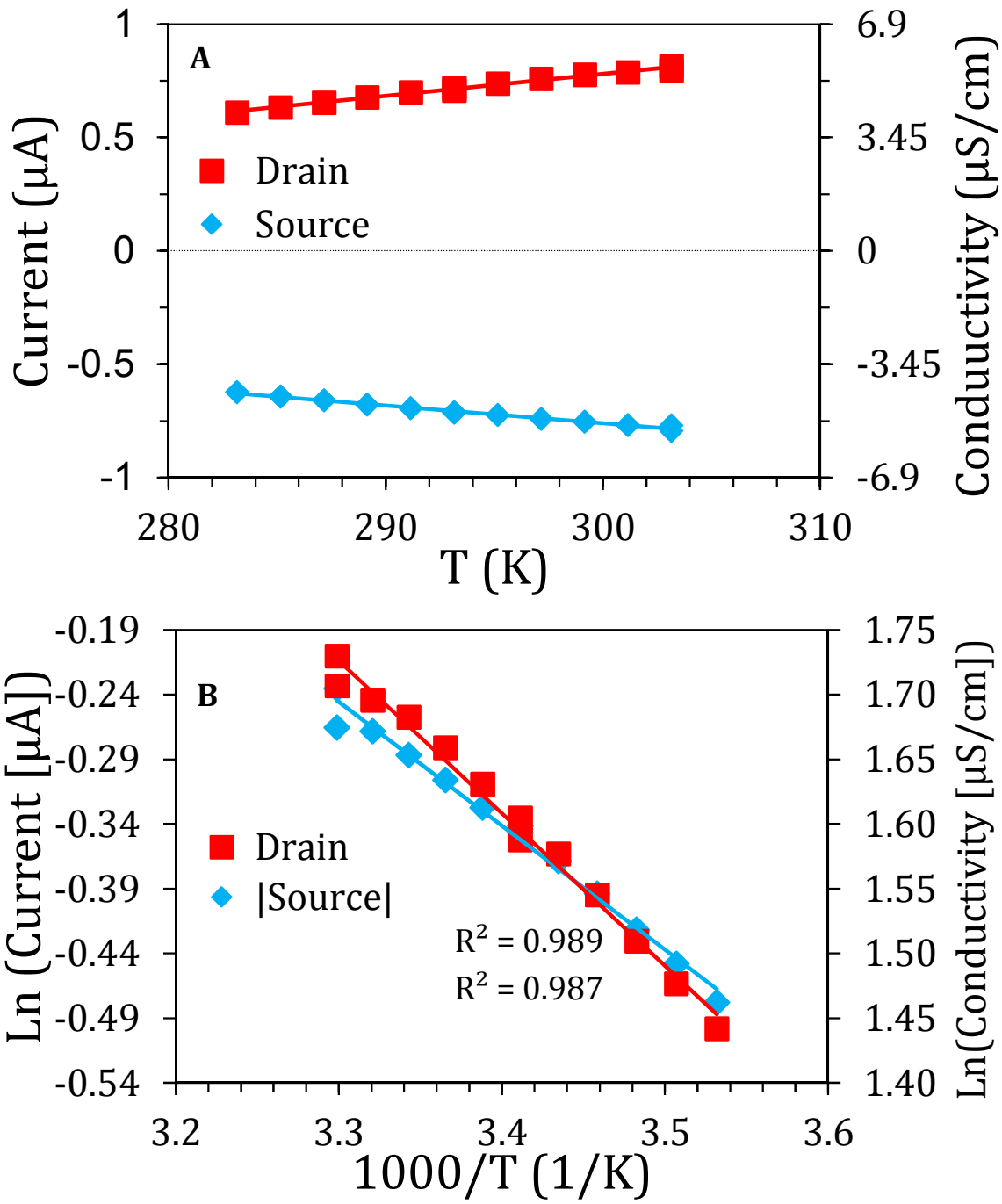


**Fig. 1**. **A:** Source-drain current ($I_{SD}$) measured separately at source and drain (left axis) and corresponding conductivity ($\sigma$, right axis) vs. temperature under non-turnover condition (no acetate present) of a living *G. sulfurreducens* biofilm grown on an interdigitated microelectrode array (IDA). Gate potential ($E_G$) is -0.390 V based on Fig. 3. Source-drain voltage ($V_{SD}$) is 0.01 V and within the linear voltage-current region. **B**: Corresponding Arrhenius plot, slope yields an activation energy ($E_a$) of 0.13 ± 0.02 eV (Eqn 7) and reorganizational energy ($\lambda$) of 0.52 ± 0.08 eV (averages of 3 replicates). The

slope was calculated using Eqn. 11. Representative data is shown here. Replicates can be found in Supplementary Information.

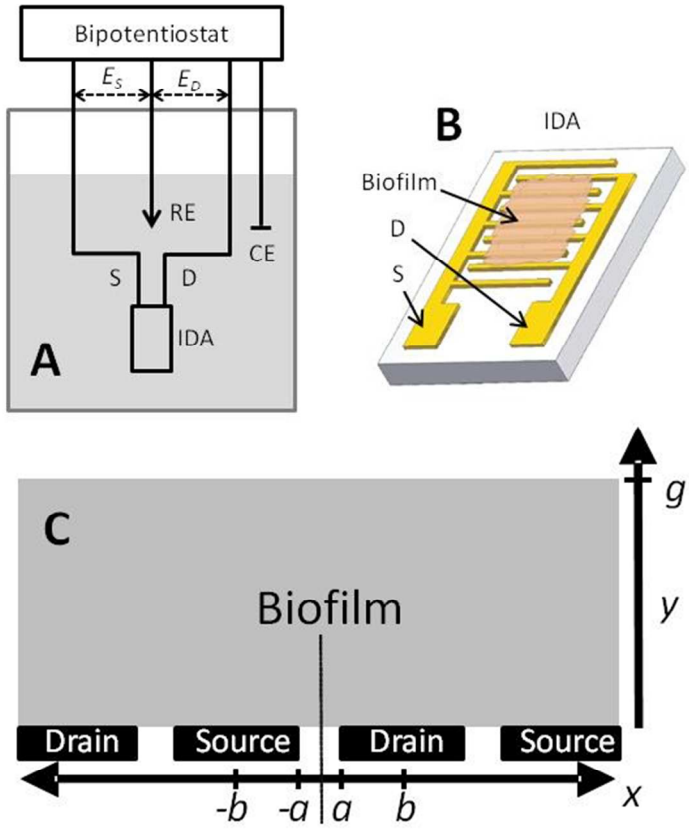


**Fig. 2.** Experimental set up. **A**: Water-jacketed 250-ml anaerobic electrochemical reactor containing freshwater medium in which a living *G. sulfurreducens* biofilm was grown on an IDA (S: source, D: drain, RE: Ag/AgCl reference electrode, CE: counter electrode). Bipotentiostat separately applies source and drain potentials ($E_S$ and $E_D$) vs. RE (gate potential, $E_G = (E_D + E_S)/2$), source-drain voltage, $V_{SD} = E_D - E_S$) and separately measures resulting source-drain current ($I_{SD}$) at each electrode. **B:** Biofilm growth confined to unmasked region of IDA comprised of alternating source and drain electrode bands. **C**: Schematic of biofilm/IDA cross-section depicting 4 alternating source and drain bands. IDAs used here contained 130 bands. IDA dimensions are provided in the Materials and Methods Section.

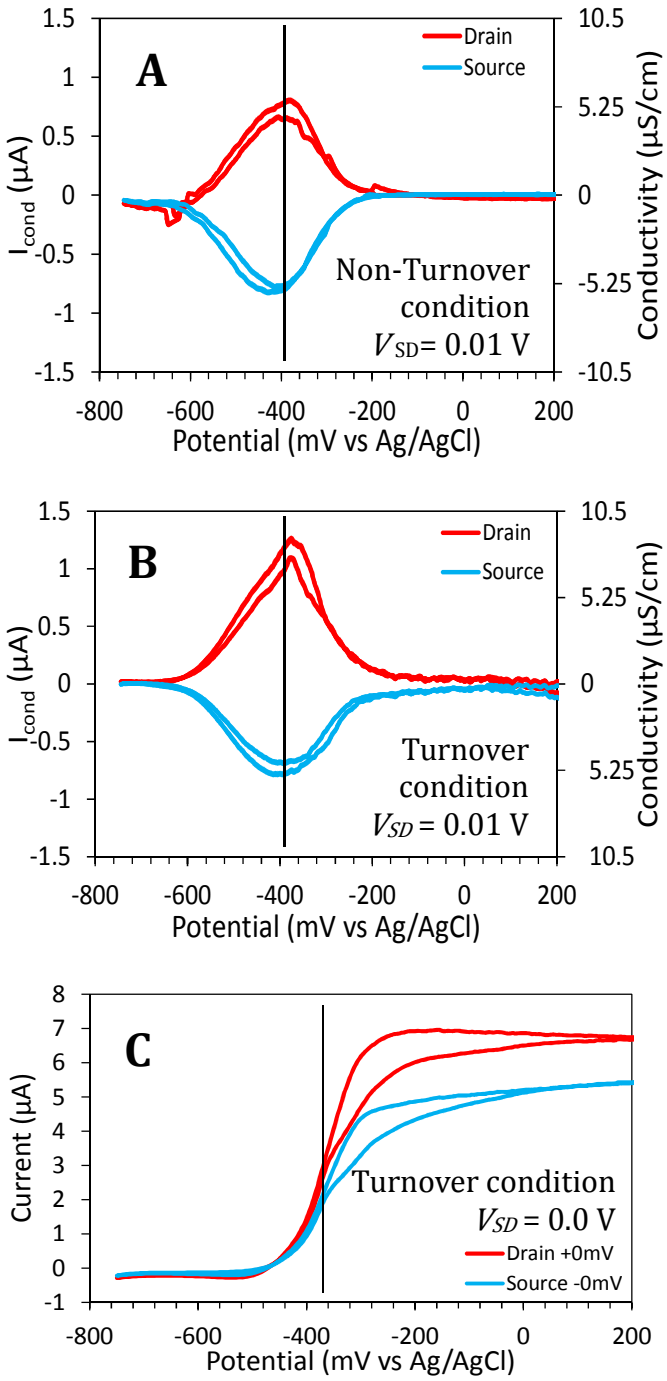


**Fig. 3.** Electrochemical gating measurements ($I_{SD}$ vs. $E_G$) for $V_{SD}$ = 0.01 V under **A:** non-turnover condition, and **B**: turnover condition. Background currents have been subtracted out (details in Materials and Methods) leaving only source-drain currents (Raw data can be found in Supplementary Information). **C**: Turnover condition, $V_{SD}$ = 0.0 V such that $I_{SD}$ = 0 (equivalent to biofilm acetate turnover (catalytic) voltammetry recorded simultaneously at each electrode) where the observed current is attributed to the sum of

acetate turnover current and Faradaic charging current. Scan rate ($v$, rate of change of $E_G$) is 1 mV/s for all three cases to approximate steady current at each value of $E_G$.

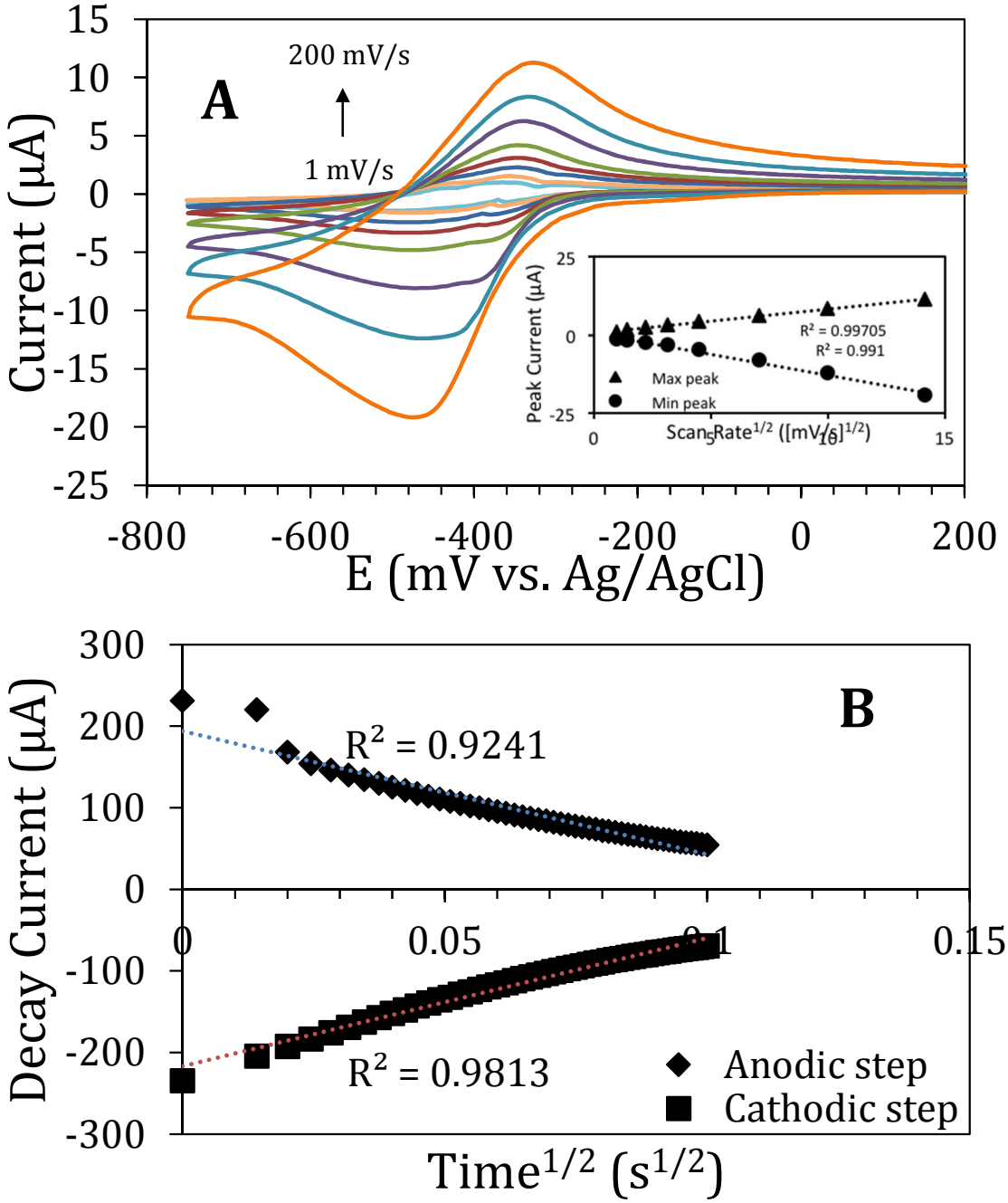


**Fig. 4. A:** Biofilm non-turn turnover voltammetry. $V_{SD}$ = 0.0 V such that $I_{SD}$ = 0. Resulting current, attributed to Faradaic charging only, depicted for different scan rates ($v$ = 1 to 200 mV/s)**. Inset**: Anodic and cathodic peak current of **A** vs. square root of scan rate. **B:** Current decay vs. square root of time following potential step from -0.65 V to -0.25 V (anodic step) and -0.25 V to -0.65 V (cathodic step) so as to rapidly covert all electrode-accessible redox cofactors in biofilm from the reduced state to the oxidized state (anodic step) and *vice versa* (cathodic step).